Vol. **113** (2008) *ACTA PHYSICA POLONICA A* No. 1

Proceedings of the CSMAG'07 Conference, Košice, July 9–12, 2007

Magnetization Reversal Processes in the Nanocrystalline Fe–Co–Zr–Ti–Pr–B Magnets

K. Pawlik, P. Pawlik, J.J. Wysłocki

Institute of Physics, Częstochowa University of Technology
Al. Armii Krajowej 19, 42-200 Częstochowa, Poland

and W. Kaszuwara

Faculty of Engineering Materials, Warsaw University of Technology
Wołoska 141 Warsaw, Poland

Magnetization reversal processes in the magnets derived from the $Fe_{60}Co_{13}Zr_1Ti_3Pr_9B_{14}$ alloy were investigated. It was shown that the processing technique affects the magnetization reversal processes. For the nanocrystalline ribbon samples pinning of the domain walls arises at low external magnetic fields while nucleation of reversed domains occurs at higher fields. However, the nucleation fields are lower than the pinning fields for the nanocrystalline rod and tube samples produced by suction-casting technique.

PACS numbers: 75.50.Ww, 75.50.Kj, 71.20.Eh

1. Introduction

The microstructure of hard magnetic materials has direct effect on the magnetic properties of the permanent magnets. This phenomenon was previously studied in [1] for sintered and melt-spun NdFeB magnets. The valuable information about the magnetization reversal mechanism can be obtained from the field dependences of reversible $M_{\rm rev}$ and irreversible $M_{\rm irr}$ parts of the magnetization determined from the recoil curves. It was shown in [2] that $M_{\rm rev}$ vs. $M_{\rm irr}$ dependences calculated at constant H are directly related to the magnetization reversal process present in magnet.

Taylor et al. [3] have shown that intergrain dipolar fields or crystallographic defects can stabilize residual areas of reversed magnetization, therefore they may impact a value of coercive field $H_{\rm c}$ and affect the reversal process [4]. Furthermore, the magnetization reversal process in nanocrystalline magnets may consist of both

nucleation of reversed domains and pinning of domain walls. Depending on the alloy composition and the microstructure, the nucleation fields H_n may be greater or smaller than pinning fields H_p.

Moreover, not identical micromagnetic conditions of the nanocrystals result in a distribution of the H_n and H_p values. Crew and Lewis [5] developed micromagnetic model to describe relation between M_{rev} and M_{irr} for the sintered NdFeB. In this model magnetically isolated identical grains were used. The state of grains is determined by the external magnetic field H and the distribution of H_n and H_p. It was shown in [5] that the M_{rev} vs. M_{irr} dependence will vary depending on values of H_p and H_n and their distributions. The aim of the present work is to study the differences in the magnetization reversal processes of nanocrystalline samples of $Fe_{60}Co_{13}Zr_1Ti_3Pr_9B_{14}$ alloy produced by various methods.

2. Experiment, results and discussion

Ingot samples of the $Fe_{60}Co_{13}Zr_1Ti_3Pr_9B_{14}$ alloy were melt-spun to ribbon at high speed of 30 m/s (≈ 20 μm of the thickness). Nanocrystalline $Pr_2(FeCo)_{14}B$ hard magnetic phase was derived by annealing the ribbon at 973 K for 10 min. 1 mm diameter rods and 3 mm outer diameter (o.d.) tubes (≈ 0.3 mm wall thickness), produced by suction-casting technique for the same alloy composition were nanocrystalline in the as-cast state. The bulk samples were annealed at 573 K for 10 min to relax the microstructure. Both processing and annealing procedures were carried out under an Ar atmosphere. The M_{rev} vs. M_{irr} dependences were determined from the recoil curves measured on initially saturated samples as described in [1], at room temperature. Furthermore, the field dependence of coercivity and initial magnetization curves were obtained from minor hysteresis loops.

It was shown previously in [6] that suction-cast rods and tubes consist of single $Pr_2(Fe,Co)_{14}B$ hard magnetic phase in as-cast state. Furthermore, the microstructure of the bulk samples contains large crystallites (diameter of ≈ 250 nm) and agglomerates of small nanocrystals (diameter < 10 nm). The ribbon samples devitrified at 973 K/10 min close to the crystallization temperature of 2-14-1 phase are also single phase nanocrystalline magnets. Therefore these magnets are good candidates for studies of magnetization reversal process. M_{rev} vs. M_{irr} dependences obtained for samples initially saturated at 5 T are shown in Fig. 1. Some differences between behaviour of bulk samples and nanocrystalline ribbons indicate substantial difference in magnetization reversal processes. For rods the M_{rev} versus M_{irr} revealed shallow minimum corresponding to positive values of irreversible magnetization at low external magnetic fields. Similar traces were obtained for the tube samples. According to model of Crew and Lewis [5], pinning fields H_p prevail nucleation fields H_n in such system or are very close to each other. Furthermore, shift of the minima of curves towards positive values of M_{irr} suggests that the nucleated domain walls are swiftly pinned just after nucleation. In case

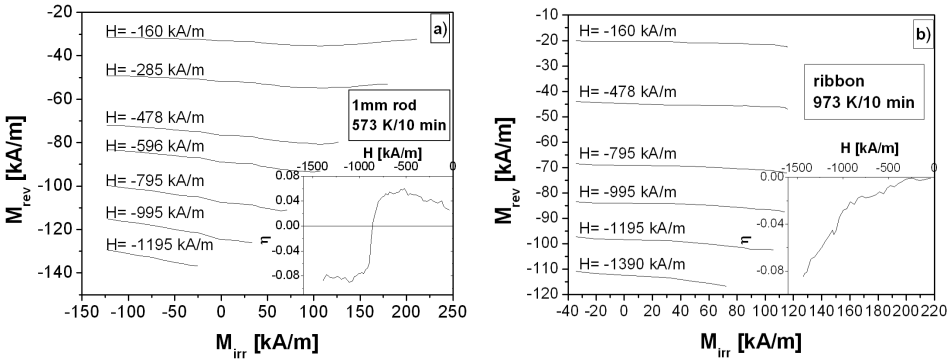

Fig. 1. Plots of $M_{\rm rev}$ vs. $M_{\rm irr}$ determined from the demagnetizing recoil curves for 1 mm diameter rod (a) annealed both at 573 K/10 min; and for (b) 20 μm thick ribbon devitrified at 973 K for 10 min.

of ribbon samples a linear decrease in $M_{\rm rev}$ with increasing $M_{\rm irr}$ was measured. The shapes of $M_{\rm rev}(M_{\rm irr})$ curves suggest that the nucleation process occurs for larger H, while pinning fields are of lower values. The dependence of the $M_{\rm rev}$ on $M_{\rm irr}$ is theoretically described by parameter [2], which is a slope of $M_{\rm rev}(M_{\rm irr})$ dependences taken for fields closest to the demagnetization curves. Plots of $\eta(H)$ are presented in the insets of Figs. 1a and b for particular sample. For rod and tube samples η reaches positive values for reversed fields lower than 860 kA/m and 600 kA/m, respectively. These fields are approximately equal to $H_{\rm c}$ of particular sample. Also the shapes of the $\eta(H)$ curves correspond to pinning of reversed domains. For the devitrified ribbon samples, η take only negative values and decrease with increasing H, which is expected for nucleation of reversed domains [5]. However, in all three cases the η parameter reach relatively low values in comparison to the pure nucleation or pinning processes. Interesting information about magnetization reversal mechanism can be obtained for samples initially in the demagnetized state, measured at low external magnetic fields. $H_{\rm c}$ dependences on the maximum magnetic field $H_{\rm max}$ (Fig. 2a) and initial magnetic polarization $J(H)$ curves (Fig. 2b) were measured on initially demagnetized samples. $H_{\rm c}(H_{\rm max})$ and $J(H)$ curves differ for bulk and for ribbon samples investigated. Furthermore, the initial susceptibility measured for the ribbon is about half of the values measured for bulk samples. For bulk samples, the reversed domains nucleate at relatively low fields $H_{\rm n}$ and subsequently are pinned at $H_{\rm p}$ of larger values. At this stage the magnetic polarization rapidly increases but reaching pinning field, J increases much slower. Similarly, the coercivity increases linearly due to the same reason until the domain walls are unpinned. In case of ribbon, pinning fields are lower than the nucleation fields, therefore coercivity is very low until the domain walls become unpinned. Subsequently the $H_{\rm c}$ increases not only due to unpinning but also owing to the nucleation of reversed domains at higher fields.

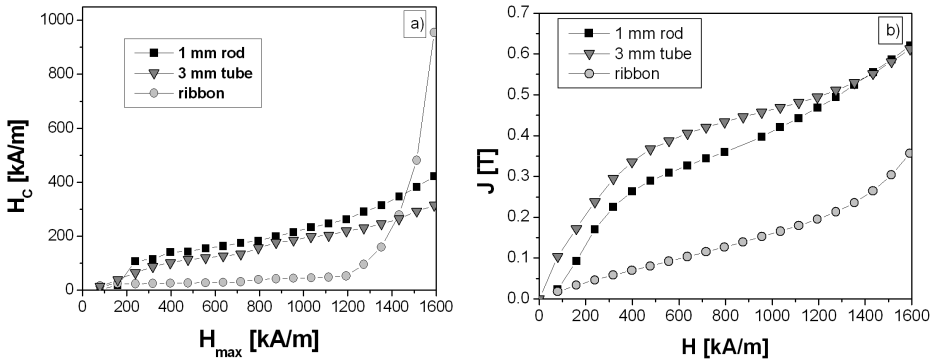

Fig. 2. H_c dependences on the maximum external magnetic field H_{max} measured at initially demagnetized state (a); initial magnetization curves (b), measured for rod, tube, and ribbon samples.

3. Conclusions

Collective mechanism comprising both pinning and nucleation processes seems to be responsible for the magnetization reversal processes observed in the investigated bulk rod and tube samples as well as in devitrified thin ribbon specimens. However, significant differences in the reversal processes between bulk and ribbon samples were shown. Complementary magnetic measurement procedures used in this work allow not only to determine the route that the reversal process proceeds, but also to compare the magnitude of pinning and nucleation fields. The differences in the magnetization reversal could be explained basing on a model using distinct distribution of nucleation and pinning fields in bulk and ribbon samples. In case of bulk samples the pinning fields prevail nucleation fields in the system, while for devitrified nanocrystalline ribbon samples the pinning fields are lower than nucleation fields.

Acknowledgments

Work supported by the Polish Ministry of Science and Higher Education (grant 3T08A 063 27).

References

[1] D.C. Crew, P.G. McCormick, R. Street, *J. Appl. Phys.* **86**, 3278 (1999).

[2] R. Cammarano, P.G. McCormick, R. Street, *J. Phys. D* **29**, 2327 (1996).

[3] D.W. Taylor, V. Villas-Boas, Q. Lu, M.F. Risignol, F.P. Missell, D. Givord, S. Hirosawa, *J. Magn. Magn. Mater.* **130**, 225 (1994).

[4] D.C. Crew, L.H. Lewis, D.O. Welch, F. Pourarian, *J. Appl. Phys.* **87**, 4744 (2000).

[5] D.C. Crew, L.H. Lewis, *J. Appl. Phys.* **87**, 4783 (2000).

[6] P. Pawlik, K. Pawlik, H.A. Davies, W. Kaszuwara, J.J. Wysłocki, N. Harrison, I. Todd, *J. Alloys Comp.* **423**, 99 (2006).